Catalysis Science & Technology

Accepted Manuscript

This article can be cited before page numbers have been issued, to do this please use: S. Rohani, A. Ziarati, G. Mohammadi Ziarani, A. Badiei and T. Bürgi, *Catal. Sci. Technol.*, 2019, DOI: 10.1039/C9CY00798A.

ROYAL SOCIETY OF CHEMISTRY

rsc.li/catalysis

View Article Online
DOI: 10.1039/C9CY00798A

Journal Name

ARTICLE

Engineering of Highly Active Au/Pd Supported on Hydrogenated Urchin-like Yolk@Shell TiO_2 for Visible Light Photocatalytic Suzuki Coupling

Received 00th January 20xx,
Accepted 00th January 20xx

DOI: 10.1039/x0xx00000x

www.rsc.org/

Sahar Rohani, [a,b] Abolfazl Ziarati, [b,c] Ghodsi Mohammadi Ziarani, [a] Alireza Badiei, [c] Thomas Burgi [b,*]

Efficient smart photocatalysts and their surface engineering are necessary for the effective conversion of light energy into chemical energy in photo-catalyzed organic reactions. Herein, we designed a hydrogenated urchin-like yolk@shell TiO_2 structure decorated with Au and Pd nanoparticles (HU@S-TOH@AuPd) as a robust photocatalyst for C-C coupling reactions. The resulting architecture exhibits a considerable photocatalytic performance in Suzuki couplings under visible light irradiation with a turnover frequency (TOF) value as high as 7095 h^{-1}. The beauty of this engineered structure is lying on the following four points; (I) the urchin-like structure provided large accessible surface area for high light harvesting as well as high noble metals anchoring; (II) the yolk@shell mesoporous architecture improved the absorption of light by multiple scattering; (III) the presence of Ti^{3+} species on the surface of TiO_2 decreased the band gap of the structure to the visible region; and (IV) the enriched electron density of Pd through the injection of hot electrons from Au as well as the flow of electrons from the titanium dioxide semi-conductor to the metals, accelerated the rate-determining step. The merging of bimetallic plasmonic nanoparticles and urchin like yolk-shell hydrogenated titanium dioxide architecture can open an avenue for designing photocatalysts with high stability and promising activity as well as high direct harvesting of visible light for a broad range of photocatalytic organic reactions.

Introduction

Development of environmentally friendly photocatalytic materials for organic molecular transformations with high activity and stability in mild conditions is of great importance for both fundamental research and practical applications.[1, 2] One special focus is on the use of the photo-induced electrons/holes for reduction/oxidation of organic molecules.[3, 4] Despite the fact that the simultaneous application of photo-excited electrons and holes for organic reactions offer a novel and promising catalytic strategy for the economical and green chemical synthesis, it is rarely reported and still a challenge for the scientific community.[5, 6] Suzuki–Miyaura coupling is one of the most powerful tools in modern organic synthesis for C–C bond formation.[7-9] Photocatalytic Suzuki reaction driven by visible light is an ideal procedure, due to its clean and abundant energy source, benign environmental impact and sustainability.[10-12]

TiO_2 nanomaterials are extensively considered to be state of the art photocatalysts for energy conversion and environmental protection.[13-15] Nevertheless, the low photocatalytic performance caused by large band gap, rapid recombination rate of photo-generated carriers and low specific surface area are challenging issues which need to be addressed to enable useful applications.[16, 17] Structure engineering is a highly promising approach for improving the optical and electronic properties of TiO_2 in the visible light region.[18] For this aim, one way is deposition of noble metal particles on the surface of titania.[19] This noble metal grafting can efficiently increase the interfacial charge transfer by formation of a ''Schottky'' barrier between titania and metal, which can be indexed to the various Fermi levels of metal and TiO_2.[20] Under visible light illumination, photo-induced electrons in the conductive band (CB) of titania can be transferred to noble metals as the Fermi level of these metal particles are located below the CB of the n-type TiO_2 semiconductor.[21]

[a] Department of Chemistry, Faculty of Science, University of Alzahra, Tehran, Iran
[b] Department of Physical Chemistry, University of Geneva, 30 Quai Ernest-Ansermet, 1211, Geneva 4, Switzerland
[c] School of Chemistry, College of Science, University of Tehran, Tehran, Iran
E-mail: Thomas.Buergi@unige.ch
Tel: +41(0)22 379 65 52
Electronic Supplementary Information (ESI) available. See DOI: 10.1039/x0xx00000x

DOI: 10.1039/C9CY00798A

On the other hand, Pd nanoparticles (NPs) play an important role in C-C bond-forming reactions due to their unique ability to activate reactants *via* the formation of metal–carbon bonds.[22] Although, Pd NPs can strongly absorb the UV and visible light through interband electronic transitions, their weak plasmonic properties inhibit the application of Pd in the plasmonic field.[12, 23, 24] With the help of the strong localized surface plasmon resonance (LSPR) of Au under light irradiation Au/Pd bimetallic nanoparticles have been proven efficient in light harvesting and as catalyst for Suzuki coupling reaction.[25-27] In this regards, several efforts have been devoted to improve the activity of heterogeneous AuPd-based TiO_2 catalysts for visible-light-induced Suzuki coupling reaction. Yan *et al.* reported a well-designed Au–TiO_x–Pd photocatalyst that indicated high performance towards Suzuki–Miyaura reactions at ambient conditions under solar irradiation.[28] Zhang and co-workers fabricated Au-Pd/TiO_2 catalyst, which exhibited high photocatalytic activity for coupling reactions of aryl boronic acids with substituted aryl halides under visible light.[24] Inspired by these reports, we tried to design an engineered Au-Pd/TiO_2 architecture to improve the photocatalytic activity in Suzuki reaction.

Among various morphologies of TiO_2, yolk–shell (Y@S) structures, composed of a movable core inside a hollow cavity enclosed by a porous outer shell, have gained much research attention due to their unique properties.[29, 30] These smart materials are conducive for photocatalysis due to relatively high surface area, high light-harvesting, low diffusion resistance and multiple light-scattering within the sphere interior voids.[30, 31] Up to date, it has been demonstrated that nanoarchitectures with hierarchical surface have enhanced features compared to those with smooth surface.[32] Among them, readily accessible urchin-like structures with properties of interconnected porous framework and high specific surface area, can increase the efficiency of light-harvesting as well as facilitate the accessibility of reactants to the active sites.[33] On the other hand, surface structure engineering has afforded many breakthroughs in enhancing the photocatalytic activity of titania through creating a defect-rich or disordered surface layer with black colour therefore improving its optical absorption in the visible region.[34, 35] The presence of oxygen vacancies on the surface of black TiO_2, provides excess electrons at the defect sites, decreases the band gap of TiO_2 to the visible region and decreases the charge recombination.[24, 36, 37]

Based on the above considerations, the design of noble metal NPs decorated yolk–shell TiO_2 structure with hydrogenated urchin-like surface is an effective method to solve the low light-harvesting efficiency of titania which can lead to the next generation of advanced photocatalytic materials for coupling reactions. Therefore, following research endeavours from our groups,[38-41] herein we wish to propose the hierarchical urchin-like yolk@shell TiO_2 architecture decorated with plasmonic Au/Pd NPs (HU@S-TOH@AuPd) as an advanced architecture for photocatalytic Suzuki-Miyaura coupling reactions at room temperature under visible light irradiation.

Results and discussion

Preparation and characterization of HUY@S-TOH/AuPd architecture

Fig. 1 illustrates the multi-step procedure for the preparation of HUY@S-TOH/AuPd nanoarchitectures. In step I, the Y@S-TO spheres are formed by one-pot solvothermal method using polyethylene glycol as soft template.[40] Next, in step II, dissolution–recrystallization process in an alkaline water/alcohol media was used to produce hierarchical urchin like shell (HUY@S-TO). In step III, the 3D HUY@S-TOH

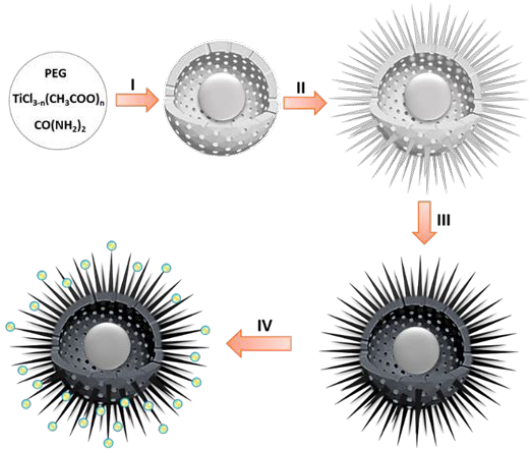

Fig. 1. Overall flowchart for the fabrication of HUY@S-TOH/AuPd architecture.

architectures were obtained by using of hydrogen treatment method.[42] Finally, the as-prepared Au/Pd core/shell NPs were decorated on the surface of HUY@S-TOH to yield HUY@S-TOH/AuPd architecture (step IV).

The SEM analysis was used to investigate the surface morphology of designed architecture. The SEM image of HUY@S-TOH/AuPd (Fig. 2a) shows the presence of urchin-like monodisperse microspheres with a diameter of ~ 3 µm. The broken sphere (yellow arrow) implies the Y@S configuration in which a movable solid core was located inside the urchin-like

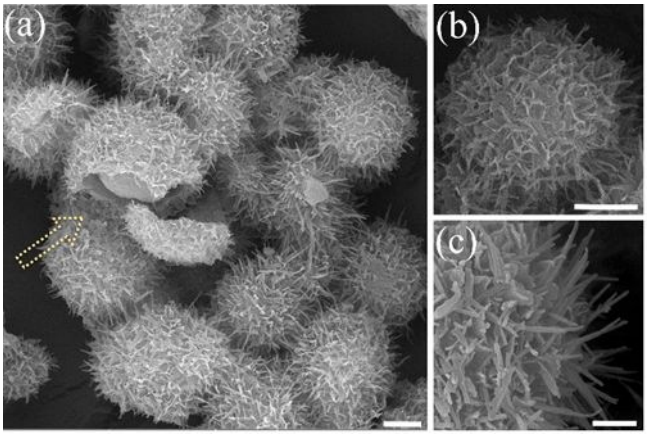

Fig. 2. SEM images of HUY@S-TOH/AuPd architecture. The scale bars are 1 µm (a, b) and 200 nm (c).

shell. From SEM images of HUY@S-TOH/AuPd in higher magnifications (Fig. 2b, c), the well-developed hairy needles assembled on the surface of microspheres are clearly seen, resulting in urchin like structures.

More detailed morphological information of the designed structures were obtained by TEM analysis in comparison with the Y@S-TO structure. The typical TEM images of Y@S-TO (Fig. 3 a-c) in different magnifications, confirmed the Y@S configuration in this structure. Moreover, the relatively smooth surface in this structure is clearly obvious (Fig. 3c). Besides, Fig. 3 (f-h) revealed hierarchical urchin-like structure

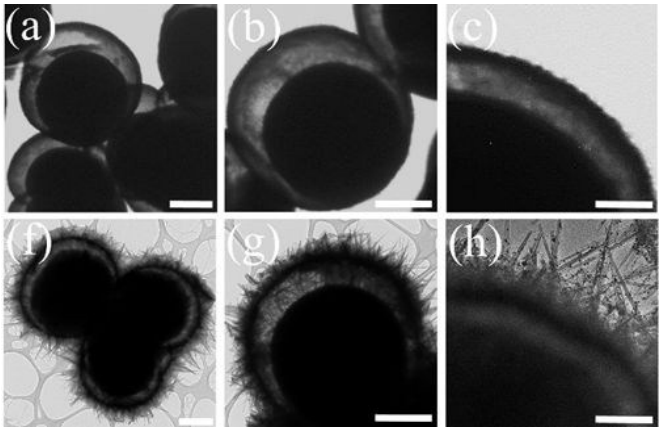

Fig. 3. TEM images of Y@S-TO (a-c) and HUY@S-TOH/AuPd (f-h). The scale bars are 1 µm (a, b, f, g), and 200 nm (c, h).

of HUY@S-TOH that was created by dissolution–recrystallization process in water/alcohol media. As can be seen in these images, the urchin-like needles were successfully assembled on the surface of Y@S structure.

High-resolution TEM (HRTEM) images of Y@S-TO (Fig. 4 a,b) and HUY@S-TOH/AuPd (Fig. 4 c, d), clearly indicate that the two structures have good crystallinity with an interplanar distance of 0.35 nm between (101) TiO_2 planes (red arrows). Meanwhile, in the case of HUY@S-TOH/AuPd architecture, a thin disordered surface layer (white arrows) owning to the effect of hydrogen treatment could be observed.[43] Additionally, in Fig. 4 (c, d) spherical AuPd NPs are evident on the surface needles of HUY@S-TOH architecture with the average diameter of ~5 nm and the lattice spacing of about 0.24 nm, which matched well with the (111) crystalline plane of Au (yellow arrows). A narrow shell on the surface of Au NPs (blue line, ca. 0.7 nm) is obvious that can be attributed to the Pd deposition and preparation of Au-Pd core/shell NPs, as later on confirmed by XPS analysis. Moreover, to better distinguish the structure of Au and Pd, the HRTEM analysis was done for pristine AuPd nanoparticles. As is clear from Fig. S1, the Au core (darker part) is covered by the Pd shell (lighter part).

Energy Dispersive X-ray Spectrometry (EDS) elemental mapping analysis was also performed to identify the elemental composition of the architecture (Fig. S2). The results reveal that the HUY@S-TOH/AuPd structure mainly contains uniform distribution of Ti, O and Au as well as Pd elements.

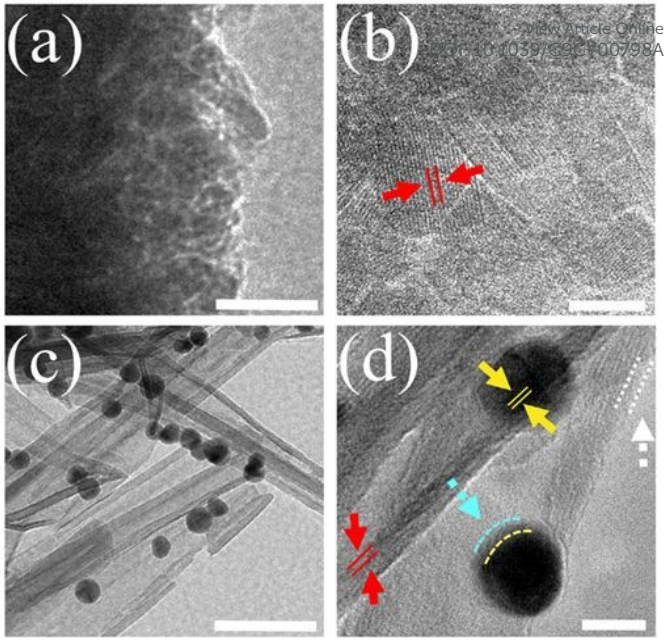

Fig. 4. HRTEM images of Y@S-TO (a, b) and HUY@S-TOH/AuPd (c, d). The scale bars are 50 nm (a, c) and 5 nm (b, d).

X-ray photoelectron spectroscopy (XPS) was used to analyze the valence states of Ti, Pd and Au in the modified HUY@S-TOH/AuPd architecture (Fig. S3). As can be seen in Fig. S3a, two bands located at binding energy (BE) of 459.0 eV and 464.9 eV were attributable to the Ti $2p_{3/2}$ and Ti $2p_{1/2}$ photoelectrons in Ti^{4+} chemical state, while two peaks at 456.9 eV and 463.2 eV were indexed to the $2p_{3/2}$ and $2p_{1/2}$ core levels of Ti^{3+} in the black TiO_2. Besides, the Au 4f and Pd 3d spectra demonstrated two contributions resulting from spin–orbit splitting. The BE peak at 83.2 eV correspond to Au $4f_{7/2}$, suggesting the presence of Au (0) species on the surface of nanoarchitecture.[44] Meanwhile, the main BE peak of Pd $3d_{5/2}$ was located at 333.7 eV, suggesting that the Pd species are in a metallic state which has been proven efficient for attaining high catalytic performance toward Suzuki coupling reaction. Remarkably, a slight positive shift relative to the typical BE of Ti $2p_{3/2}$ at 459.0 eV and also a negative shift of the typical BE for Au (0) and Pd (0) at 84.0 eV and 335.0 eV, respectively, can be attributed to the transfer of electrons from the titania to the Au/Pd core/shell nanospheres.[24, 45, 46] These electron flows can enhance the electron density around Pd particles which can accelerate the Suzuki reaction. Besides, the weight amount of the Au and Pd species in the engineered HUY@S-TOH/AuPd structure, determined by XPS analysis, are ~ 2.3 and 0.6 wt% respectively.

The XRD and DRS analysis of Y@S-TO, HUY@S-TOH and HUY@S-TOH/AuPd were also performed (Fig. S4). The XRD patterns confirmed that all architectures possess a good crystallinity with the well-defined tetragonal anatase structure of TiO_2 (JCPDS No. 21-1272). After hydrogenation, a slight shift to higher diffraction angles was observed in HUY@S-TOH which can be attributed to the reduction of the interplanar spacing of crystalline titania phase.[47] In the engineered

HUY@S-TOH/AuPd structure, all reflections are preserved, implying that the decoration with Au–Pd NPs has no effect on the crystal phase of the TiO_2 support. Moreover, two small reflections could be observed at ~38˚ and 44˚, for (111) and (200) planes of Au, respectively (JCPDS: 10-0784). No distinct diffraction peaks ascribed to Pd are distinguished, because of the size of Pd shell deposited on the surface of Au core is lower than the detection limit of XRD analysis (<4 nm). Evidence for the formation of Ti^{+3} and Au–Pd core-shell NPs on the engineered structure was also seen by UV-vis diffuse reflectance spectra (DRS) in which the HUY@S-TOH/AuPd architecture clearly demonstrated different features from HUY@S-TOH and Y@S-TO structures. As shown in Fig. S5, Y@S-TO displayed great light adsorption at wavelengths above 400 nm. In contrast, the spectrum of HUY@S-TOH demonstrates significant absorption of visible light that may be due to the presence of Ti^{3+} ions on the surface of structure. After decorating with Au-Pd, even stronger absorption in visible region was observed for the modified HUY@S-TOH/AuPd architecture. The strong peak at ~532 nm is owning to the LSPR effect of the core/shell Au-Pd NPs.[46]

N_2 adsorption-desorption measurement was utilized to investigate the porous structure and pore size distribution of HUY@S-TOH/AuPd sample (Fig. S6). Unlike P25, which is not mesoporous, for Y@S-TO and HUY@S-TOH/AuPd architectures, typical IV isotherms are observed, indicating the presence of mesopores in these structures. Thanks to the advantage of urchin-like surface as well as Y@S structure, the BET surface area of HUY@S-TOH/AuPd (306 $m^2 .g^{-1}$) is nearly two times larger than that of Y@S-TO (181 $m^2 .g^{-1}$) and much larger than P25 (41 $m^2 .g^{-1}$). This high surface area is desirable for great adsorption of organic substrates and efficient anchoring of AuPd NPs leads to improved photocatalytic coupling reaction. According to Barrett-Joyner-Halenda (BJH) analysis, the HUY@S-TOH/AuPd structure presented a narrow pore-size distribution in the range of 2−8 nm (Fig. S7).

3.2. Photocatalytic investigations

The influence of some critical reaction conditions in the Suzuki coupling, has been investigated by using of HUY@S-TOH/AuPd photocatalyst under a 300 W Xenon lamp irradiation, as simulated sunlight, at room temperature. The Suzuki reaction between 4-iodotoluene with phenylboronic acid, as model reaction, did not proceed in the dark (Table S1, entry 1) and at 80 °C (in the dark) a moderate yield (68%) of corresponding product was observed, (Table S1, entry 2), indicating the significant influence of irradiation on the catalytic performance. Among several solvents that were used for the reaction, the polar aprotic solvents, such as DMF and DMSO, gave low yield of the product and the nonpolar solvent, toluene, also afforded a trace yield (Table S1, entries 3-5). In contrast, higher yield of product was observed in the polar protic solvents like ethanol and methanol (Table S1, entries 6, 7). In addition, the reactions in pure H_2O hardly proceeded because of the poor solubility of 4-iodotoluene at room temperature (Table S1, entry 8); however, a mixture of protic EtOH and H_2O led to a profound increase in catalytic activity (Table S1, entry 13). This result is very different from that obtained in conventional Suzuki coupling reactions catalyzed by heterogeneous catalysts. Generally, polar DMSO and DMF are considered to be good solvents for Suzuki coupling, leading to the generation of the corresponding products in high yields. Nevertheless, this is not the case for photo-catalyzed Suzuki coupling reactions. Additionally, another protic organic solvent mixture involving MeOH gave moderate yields of the desired product in this photocatalyzed coupling reaction. These results confirmed that protic solvents play a crucial role in photocatalyzed Suzuki reactions over HUY@S-TOH/AuPd nanocatalyst. It is guessed that protic solvents may be oxidized more easily through photo-generated holes transferred from Y@S-TO. In contrast, aprotic solvents, like DMSO and DMF could not be oxidized by this hole transfer since they have higher oxidation potentials.[48] Subsequently, the effects of various bases in the mixture of EtOH:H_2O were investigated and the best result was obtained using K_2CO_3 (Table S1, entry 13). Moreover, the reaction did not proceed without the base (Table S1, entry 15), as it is necessary to activate the phenylboronic acid and it is facilitating the trans-metalation step.[49] Besides, different loadings of Au/Pd nanoparticles on the HUY@S-TOH architecture were investigated in the Suzuki model reaction (Fig. S8). As emerges from the data, the best result was obtain using 3 wt% of Au/Pd. By increasing the metal loading beyond 3 wt%, no considerable improvements in product yields were observed. To obtain better insights of HUY@S-TOH/AuPd nanoarchitecture efficiency, its photocatalytic activity in the model reaction under optimized conditions was compared with P-25, P-25/AuPd, Y@S-TO/AuPd, HUY@S-TOH/Au, HUY@S-TOH/Pd and HUY@S-TOH/AuPd structures. As can be seen in Fig. S9, by using of P-25, the reaction did not proceed at all probably due to the lack of visible light activity as well as the absence of metal NPs in this structure. However, the activity of catalyst is significantly improved with decoration of Au-Pd nanoparticles on the structures, so that the yield of reaction increased to 69% and 78% after 1h using P-25/AuPd and Y@S-TO/AuPd, respectively. The higher photocatalytic activity of Y@S-TO/AuPd compared to P25/AuPd can be ascribed to the higher surface area and better light harvesting ability, provided by yolk/shell structure in Y@S-TO/AuPd. By using monometallic structures, HUY@S-TOH/Au gave only little product (17%) and HUY@S-TOH/Pd demonstrated inferior activity compared with HUY@S-TOH/AuPd, as the yield of product was only 43%. This implies that the presence of both Au and Pd plays an important role in this photocatalytic reaction. Interestingly, the highest photocatalytic activity was observed using HUY@S-TOH/AuPd architecture with a product yield of 94% in 1h. This considerable activity can be attributed to the hydrogenated visible light active structure containing Ti^{3+} species on the surface of TiO_2. The latter enhance the light harvesting

efficiency of photocatalysts through inhibition of the recombination of photo-generated electrons and holes by decreasing the band gap of TiO_2 into the visible region. Furthermore, scattering of light on the hierarchical surface and between inner core and outer shell in urchin-like Y@S structure can enhance the light harvesting efficiency. Moreover, the results indicate the strong interaction between noble metals and TiO_{2-x}. Electron transfer between Ti^{3+} and metal particles, as previously verified by XPS analysis, leads to an electron-rich Pd surface, which finally increases the catalytic performance of this architecture.[50] These results clearly demonstrate the high activity of the used urchin-like hydrogenated HUY@S-TOH/AuPd nanoarchitecture for photocatalytic Suzuki coupling reaction.The reaction protocol was further extended in the coupling of different aryl halides and phenylboronic acids to confirm the scope of catalytic system by HUY@S-TOH/AuPd under visible light irradiation (Table 1). As expected, in the case of aryl iodides, the corresponding biaryls were obtained in higher yield than aryl bromides and chlorides due to the weaker C–I bond. Moreover, the electronic nature of the substituents on the phenyl rings can affect the yield of desired products. Aryl halides with electron withdrawing substituents exhibited higher product yields as compared to those with electron donating ones. This result is reasonable, since the electron withdrawing substituents result in electron deficient aromatic ring which facilitates the nucleophilic attack *via* the photo-induced electrons on electron-rich Pd NPs. To better visualize the effect of different aryl halides on the reaction rate of Suzuki coupling, the yield of some bromobenzenes *vs* Hammett's parameter are shown in Fig. S10. To avoid complications by steric hindrance effects, Hammett plot is done for substituents in the *para*-position. As expected, in the presence of electron-withdrawing groups at para-substituted bromobenzenes, the yield of biphenyls were enhanced. [51, 52] These results are concurrent when correlated with the Hammett parameter values. [53]

Table 1. Scope of Suzuki coupling reaction catalyzed by HUY@S-TOH/AuPd under visible-light irradiation. [a]

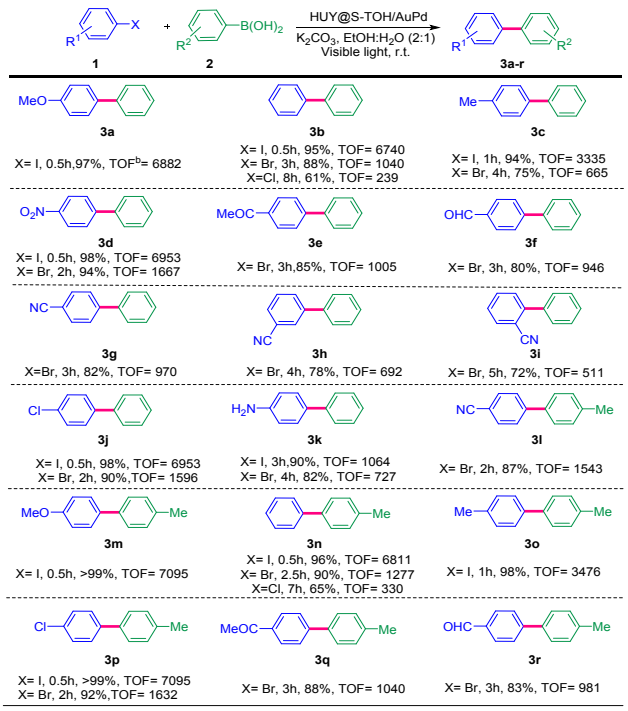

[a] Reaction conditions: arylhalide (1.0 mmol), phenylboronic acids (1.5 mmol), HUY@S-TOH/AuPd catalyst (5 mg), K_2CO_3 (2 mmol) and EtOH:H_2O (6 mL), Xe lamp, water bath, room temperature. Yields are referred to isolated pure compounds.

[b] TOF (h^{-1}) is calculated based on the yield of products and mole of Pd used.

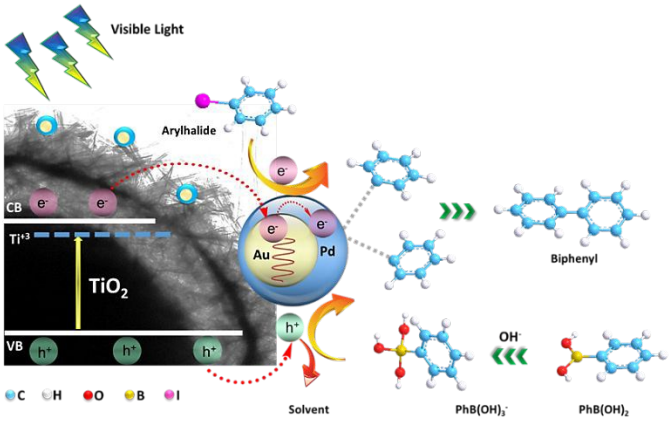

Fig. 5. Plausible mechanism for the visible light induced photocatalytic Suzuki–Miyaura coupling reaction using HUY@S-TOH/AuPd.

Furthermore, *meta*-substituted arylhalides showed lower activity than those with *para*- and *ortho*-substituents, probably a consequence of both steric hindrance and electronic effect (Table 1, 3i-k).

To get insight into the mechanism responsible for photocatalyzed Suzuki reaction using HUY@S-TOH/AuPd architecture, the coupling of 4-iodotoluene with phenylboronic acid in the presence of electron and hole scavengers were studied. 5,5-dimethyl-1-pyrroline *N*-oxide (DMPO) was used as the electron scavenger to trap the electrons from Pd, which can activate the 4-iodotoluene.[54] By addition of DMPO, no desired product was observed, suggesting that the coupling

reaction could not proceed without the reduction by the electrons from Pd. Next, the role of photo-generated holes from nanoarchitecture was investigated. Phenylboronic acid can combine with OH^- ions in basic solution and in principle adsorb on TiO_2 *via* electrostatic interaction. The photo-induced holes can diffuse to the adsorption sites of phenylboronic acid, the adsorbed molecules could be oxidized with the cleavage of C–B bond.[28] Therefore, phenylboronic acid can be activated *via* photo-generated holes under visible light illumination. To demonstrate this, triethanolamine (TEOA) as the hole scavenger, was used in the same reaction. It was observed that the reaction was quenched. Even though these results demonstrate the importance of the electron–hole pair in the photocatalytic Suzuki reaction, the exact role of holes is not yet clear.[55, 56]

Based on the above experimental results and mechanistic studies, a plausible photocatalytic mechanism can be proposed for the Suzuki–Miyaura coupling over the HUY@S-TOH/AuPd photocatalyst (Fig. 5). Under the irradiation of visible light, hydrogenated titania can absorb part of the visible light and produce electron-hole pairs. The photo-induced electrons can be injected into Au/Pd nanoparticles.[57] In parallel, the produced hot electrons, resulting from strong LSPR effect of Au, could be injected into Pd shell to increase the electron density of Pd.[58] Subsequently, the electron-rich Pd NPs can activate C–X bond of aryl halide and facilitate the oxidative addition step that seems to be the rate-determining step of the Suzuki reaction. On the other hand, the photo-generated holes can transfer to protic organic solvent, such as EtOH, or can activate the phenylboronic acid by cleaving the C–B bonds.[56, 59] While the oxidized phenyl boronic acids transfer to the activated aryl halides, the cross-coupling reaction occurs to produce the desired products *via* reductive elimination.

The photo-stability and reusability tests, as important characteristics in photocatalytic reactions, were performed to explore the stability of designed architecture. After photocatalytic Suzuki coupling of 4-iodoanisole and phenylboronic acid, the HUY@S-TOH/AuPd photocatalyst was separated from the reaction solution by centrifugation, washed with hot EtOH, and then reused for the same reaction. As becomes clear from Fig. 6, the nanoarchitecture indicated high catalytic performance for six cycles without significant loss of activity (every run is complete during 30 min).

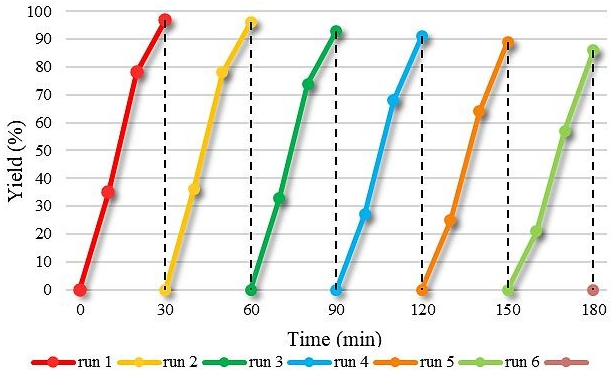

Fig. 6. Reusability study of HUY@S-TOH/AuPd in the photocatalytic Suzuki coupling reaction of 4-iodoanisole and phenylboronic acid.

A comparison reveals the highest TOF for the engineered HUY@S-TOH/AuPd nanoarchitecture in the photocatalytic Suzuki reaction with respect to other reports. As can be seen in Fig. 7 and Table S1, [24, 28, 54-57, 59-64] our catalyst remained the best performer reported yet (TOF = 7095 h^{-1}). The good performance of hydrogenated visible light active architecture can be attributed to the urchin-like surface structure that provide more accessible surface area for higher Au-Pd anchoring, prevent the agglomeration of Pd species during catalytic cycles.

Conclusions

In conclusion, we report an engineered design for the synthesis of HUY@S-TOH/AuPd architecture that demonstrated excellent photocatalytic activity in the visible-light-promoted Suzuki coupling reactions under ambient conditions. The improved activity of catalyst can be attributed to the hierarchical structure with high accessible surface area, high anchoring sites for Au/Pd, efficient light harvesting in urchin-like Y@S structure, and considerable photon absorption efficiency of visible light due to existence of oxygen vacancy as well as noble metals NPs. Moreover, the cooperative promoting effects between plasmonic Au and Pd NPs is an effective way for transferring energetic electrons from gold to palladium, by LSPR effect. A mechanistic investigation of photocatalytic Suzuki reaction suggested that photo-induced holes are transferred into EtOH or phenylboronic acid, whereas photo-generated electrons are injected to Pd NPs which can accelerate the coupling reaction. This synthetic approach for structuring Au/Pd NPs on the surface of hydrogenated titania in advanced architectures can be extended to rational design of structures with greatly improved photocatalytic activity for various energy applications and also other cross-coupling reactions using visible light.

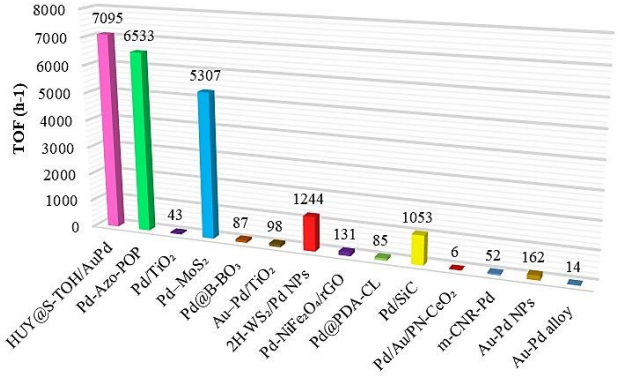

Fig. 7. Comparison of the maximum TOF value of HUY@S-TOH/AuPd with those of previously published for visible-light Suzuki reactions.

Conflicts of interest

There are no conflicts to declare.

Acknowledgements

The financial support from the research council of Alzahra University, University of Geneva, and the University of Tehran are gratefully acknowledged. SR would like to thank Ani Baghdasaryan for her help in NMR measurements.

References

1. X. Lang, X. Chen and J. Zhao, *Chem. Soc. Rev.,* 2014, **43**, 473-486.
2. M. Parasram and V. Gevorgyan, *Chem. Soc. Rev.,* 2017, **46**, 6227-6240.
3. J. C. Colmenares and R. Luque, *Chem. Soc. Rev.,* 2014, **43**, 765-778.
4. X.-H. Li, J.-S. Chen, X. Wang, J. Sun and M. Antonietti, *J. Am. Chem. Soc.,* 2011, **133**, 8074-8077.
5. C. C. Nguyen, N. N. Vu and T.-O. Do, *J. Mater. Chem. A*, 2015, **3**, 18345-18359.
6. J. Kou, C. Lu, J. Wang, Y. Chen, Z. Xu and R. S. Varma, *Chem. Rev.,* 2017, **117**, 1445-1514.
7. N. Miyaura, K. Yamada and A. Suzuki, *Tetrahedron Lett.*, 1979, **20**, 3437-3440.
8. N. Miyaura and A. Suzuki, *Chem. Rev.,* 1995, **95**, 2457-2483.
9. A. J. Lennox and G. C. Lloyd-Jones, *Chem. Soc. Rev.*, 2014, **43**, 412-443.
10. Q. Wu, P. Ju, S. Wu, Q. Su, X. Li, Z. Liu and G. Li, *J. Mater. Chem. A*, 2019.
11. H. H. Shin, T. Han, W. Yang and D.-K. Lim, *Carbon*, 2019, **143**, 362-370.
12. Y. Zhang, S. He, W. Guo, Y. Hu, J. Huang, J. R. Mulcahy and W. D. Wei, *Chem. Rev.,* 2017, **118**, 2927-2954.
13. M. Pelaez, N. T. Nolan, S. C. Pillai, M. K. Seery, P. Falaras, A. G. Kontos, P. S. Dunlop, J. W. Hamilton, J. A. Byrne and K. O'shea, *Appl. Catal. B: Environ.*, 2012, **125**, 331-349.
14. J. Schneider, M. Matsuoka, M. Takeuchi, J. Zhang, Y. Horiuchi, M. Anpo and D. W. Bahnemann, *Chem. Rev.,* 2014, **114**, 9919-9986.
15. D. Ma, A. Liu, S. Li, C. Lu and C. Chen, *Catal. Sci. Technol.,* 2018, **8**, 2030-2045.
16. W. Fang, M. Xing and J. Zhang, *J. Photochem. Photobiol.,* 2017, **32**, 21-39.
17. M. Ge, C. Cao, J. Huang, S. Li, Z. Chen, K.-Q. Zhang, S. Al-Deyab and Y. Lai, *J. Mater. Chem. A*, 2016, **4**, 6772-6801.
18. M. Nasr, C. Eid, R. Habchi, P. Miele and M. Bechelany, *ChemSusChem*, 2018, **11**, 3023-3047.
19. Y. Chen, Y. Wang, W. Li, Q. Yang, Q. Hou, L. Wei, L. Liu, F. Huang and M. Ju, *Appl. Catal. B: Environ.,* 2017, **210**, 352-367.
20. O. Ola and M. M. Maroto-Valer, *J. Photochem. Photobiol. C*, 2015, **24**, 16-42.
21. J. B. Joo, H. Liu, Y. J. Lee, M. Dahl, H. Yu, F. Zaera and Y. Yin, *Catal. Today*, 2016, **264**, 261-269.
22. A. Biffis, P. Centomo, A. Del Zotto and M. Zecca, *Chem. Rev.,* 2018, **118**, 2249-2295.
23. T. Pakizeh, *J. Opt.*, 2012, **15**, 025001.
24. D. Han, Z. Bao, H. Xing, Y. Yang, Q. Ren and Z. Zhang, *Nanoscale*, 2017, **9**, 6026-6032.
25. K. D. Gilroy, A. Ruditskiy, H.-C. Peng, D. Qin and Y. Xia, *Chem. Rev.,* 2016, **116**, 10414-10472.
26. M. Wen, S. Takakura, K. Fuku, K. Mori and H. Yamashita, *Catal. Today*, 2015, **242**, 381-385.
27. N. A. Nemygina, L. Z. Nikoshvili, I. Y. Tiamina, A. V. Bykov, I. S. Smirnov, T. LaGrange, Z. Kaszkur, V. G. Matveeva, E. M. Sulman and L. Kiwi-Minsker, *Org. Process Res. Dev.*, 2018, **22**, 1606-1613.
28. F. Wang, C. Li, H. Chen, R. Jiang, L.-D. Sun, Q. Li, J. Wang, J. C. Yu and C.-H. Yan, *J. Am. Chem. Soc.*, 2013, **135**, 5588-5601.
29. R. Purbia and S. Paria, *Nanoscale*, 2015, **7**, 19789-19873.
30. J. Liu, S. Z. Qiao, J. S. Chen, X. W. D. Lou, X. Xing and G. Q. M. Lu, *Chem. Commun.*, 2011, **47**, 12578-12591.
31. Z. Li, M. Li, Z. Bian, Y. Kathiraser and S. Kawi, *Appl. Catal. B: Environ.*, 2016, **188**, 324-341.
32. X. Li, J. Yu and M. Jaroniec, *Chem. Soc. Rev.,* 2016, **45**, 2603-2636.
33. J. Jiang, Z. Xing, M. Li, Z. Li, X. Wu, M. Hu, J. Wan, N. Wang, A. S. Besov and W. Zhou, *Ind. Eng. Chem. Res.*, 2017, **56**, 7948-7956.
34. W. Zhou, W. Li, J.-Q. Wang, Y. Qu, Y. Yang, Y. Xie, K. Zhang, L. Wang, H. Fu and D. Zhao, *J. Am. Chem. Soc.,* 2014, **136**, 9280-9283.
35. L.-B. Xiong, J.-L. Li, B. Yang and Y. Yu, *J. Nanomater.*, 2012, **2012**, 9.
36. A. Ziarati, A. Badiei and R. Luque, *Appl. Catal. B: Environ.*, 2018, **238**, 177-183.
37. X. Chen, L. Liu and F. Huang, *Chem. Soc. Rev.,* 2015, **44**, 1861-1885.
38. S. Rohani, G. Mohammadi Ziarani, A. Badiei, A. Ziarati, M. Jafari and A. Shayesteh, *Appl. Organomet. Chem.*, 2018, e4397.
39. A. Ziarati, A. Badiei, R. Grillo and T. Burgi, *ACS Appl. Mater. Interfaces*, 2019, **11**, 5903-5910
40. A. Ziarati, A. Badiei, R. Luque and W. Ouyang, *J. Mater. Chem. A*, 2018, **6**, 8962-8968.
41. A. Ziarati, A. Badiei and R. Luque, *Appl. Catal. B: Environ.*, 2019, **240**, 72-78.
42. D. Chen, C. Li, H. Liu, F. Ye and J. Yang, *Sci. rep.*, 2015, **5**, 11949.
43. X. Chen, L. Liu, Y. Y. Peter and S. S. Mao, *Science*, 2011, 1200448.
44. P. Saikia, A. T MIAH and P. P. Das, *J. Chem. Sci.*, 2017, **129**, 81-93.
45. A. Cybula, J. B. Priebe, M.-M. Pohl, J. W. Sobczak, M. Schneider, A. Zielińska-Jurek, A. Brückner and A. Zaleska, *Appl. Catal. B: Environ.,* 2014, **152**, 202-211.
46. C. Han, L. Wu, L. Ge, Y. Li and Z. Zhao, *Carbon*, 2015, **92**, 31-40.
47. T. Xia and X. Chen, *J. Mater. Chem. A*, 2013, **1**, 2983-2989.
48. O. R. Luca, J. L. Gustafson, S. M. Maddox, A. Q. Fenwick and D. C. Smith, *Org. Chem. Front.*, 2015, **2**, 823-848.
49. Y. Q. Zou, J. R. Chen, X. P. Liu, L. Q. Lu, R. L. Davis, K. A. Jørgensen and W. J. Xiao, *Angew. Chem. Int. Ed.*, 2012, **124**, 808-812.
50. X. Yuan, X. Wang, X. Liu, H. Ge, G. Yin, C. Dong and F. Huang, *ACS appl. mater. interfaces*, 2016, **8**, 27654-27660.
51. F. Estudiante-Negrete, S. Hernández-Ortega and D. Morales-Morales, *Inorganica Chim. Acta*, 2012, **387**, 58-63.
52. J. R. Pioquinto-Mendoza, P. Conelly-Espinosa, R. Reyes-Martínez, R. A. Toscano, J. M. Germán-Acacio, A. Avila-Sorrosa, O. Baldovino-Pantaleón and D. Morales-Morales, *J. Organomet. Chem.*, 2015, **797**, 153-158.
53. C. Hansch, A. Leo and R. Taft, *Chem. Rev.,* 1991, **91**, 165-195.
54. Z. Jiao, Z. Zhai, X. Guo and X.-Y. Guo, *J. Phys. Chem. C*, 2015, **119**, 3238-3243.
55. X.-H. Li, M. Baar, S. Blechert and M. Antonietti, *Sci. Rep.*, 2013, **3**, 1743.
56. F. Raza, D. Yim, J. H. Park, H.-I. Kim, S.-J. Jeon and J.-H. Kim, *J. Am. Chem. Soc.*, 2017, **139**, 14767-14774.
57. S. Zhang, C. Chang, Z. Huang, Y. Ma, W. Gao, J. Li and Y. Qu, *ACS Catal.*, 2015, **5**, 6481-6488.
58. P. Verma, Y. Kuwahara, K. Mori and H. Yamashita, *J. Mater. Chem. A*, 2016, **4**, 10142-10150.
59. H. H. Shin, E. Kang, H. Park, T. Han, C.-H. Lee and D.-K. Lim, *J. Mater. Chem. A*, 2017, **5**, 24965-24971.
60. J. Chakraborty, I. Nath and F. Verpoort, *Chem. Eng. J.*, 2019, **358**, 580-588.
61. Z. J. Wang, S. Ghasimi, K. Landfester and K. A. Zhang, *Chem. Mater.*, 2015, **27**, 1921-1924.
62. Y. Li, Z. Zhang, L. Pei, X. Li, T. Fan, J. Ji, J. Shen and M. Ye, *Appl. Catal. B: Environ.*, 2016, **190**, 1-11.
63. A. Xie, K. Zhang, F. Wu, N. Wang, Y. Wang and M. Wang, *Catal. Sci. Technol.*, 2016, **6**, 1764-1771.
64. Q. Xiao, S. Sarina, E. Jaatinen, J. Jia, D. P. Arnold, H. Liu and H. Zhu, *Green Chem.*, 2014, **16**, 4272-4285.

View Article Online
DOI: 10.1039/C9CY00798A

TOC entry

Engineering of Highly Active Au/Pd Supported on Hydrogenated Urchin-like Yolk@Shell TiO_2 for Visible Light Photocatalytic Suzuki Coupling

Sahar Rohani, [a,b] Abolfazl Ziarati, [b,c] Ghodsi Mohammadi Ziarani, [a] Alireza Badiei, [c] Thomas Burgi [b,*]

Engineered hydrogenated urchin-like yolk@shell TiO_2 decorated with Au/Pd nanoparticles were designed via sequential steps and employed in visible light photocatalytic Suzuki coupling.